Cloud-driven Changes in Aerosol Optical Properties – Final Technical Report

Principal Investigators:
John A. Ogren**,** NOAA/CMDL, Boulder, CO 80305
Patrick J. Sheridan, NOAA/CMDL, Boulder, CO 80305
Co-Investigator:
Elisabeth Andrews, University of Colorado, CIRES, Boulder CO 80305

Acknowledgments:
University of Manchester (Holme Moss AMS and meteorology data)
PNNL (loan of instrumentation for all 3 field campaigns – ASP infrastructure)

Date: September 30, 2007

Abstract:

The optical properties of aerosol particles are the controlling factors in determining direct aerosol radiative forcing. These optical properties depend on the chemical composition and size distribution of the aerosol particles, which can change due to various processes during the particles' lifetime in the atmosphere. Over the course of this project we have studied how cloud processing of atmospheric aerosol changes the aerosol optical properties. A counterflow virtual impactor was used to separate cloud drops from interstitial aerosol and parallel aerosol systems were used to measure the optical properties of the interstitial and cloud-scavenged aerosol. Specifically, aerosol light scattering, back-scattering and absorption were measured and used to derive radiatively significant parameters such as aerosol single scattering albedo and backscatter fraction for cloud-scavenged and interstitial aerosol. This data allows us to demonstrate that the radiative properties of cloud-processed aerosol can be quite different than pre-cloud aerosol. These differences can be used to improve the parameterization of aerosol forcing in climate models.

Cloud-driven Changes in Aerosol Optical Properties

Fair is foul, and foul is fair:
Hover through the fog and filthy air.
Macbeth: I,i, Shakespeare

1. Introduction/Background

In addition to their detrimental effects on human health and environmental aesthetics, atmospheric particles scatter and absorb solar radiation and can thus directly affect climate. The direct radiative effect of aerosol particles (i.e., the radiative flux change per unit aerosol optical depth) is potentially equal in magnitude but opposite in sign to that of greenhouse gases (IPCC, 2001). The direct radiative forcing by aerosols is controlled both by the concentration of particles in the atmosphere and by the optical characteristics of those particles. Cloud scavenging is the major removal mechanism for anthropogenic aerosols and the scavenging efficiency depends on the size and chemical composition of the particles. Likewise, aerosol optical properties are controlled by particle size and chemical composition. The strength of direct and indirect aerosol forcing depends, in part, on the partitioning in clouds of interstitial and cloud-scavenged particles. Because of the relatively long lifetime of interstitial aerosol compared to cloud-scavenged particles, the direct forcing related to interstitial aerosol can impact a larger region. Alternatively, particles which are scavenged or nucleate to droplets impact indirect forcing through higher cloud droplet numbers, smaller cloud droplet size, and subsequent higher cloud albedo and longer cloud lifetimes.

We hypothesize that differential cloud scavenging (i.e., preferential removal of an aerosol type based on its inherent characteristics such as size or composition) causes systematic changes in aerosol optical properties. Through a series of experiments we evaluate the magnitude of those

changes for different aerosol types. In on-going collaboration with other ASP investigators, the processes controlling differential cloud scavenging are being diagnosed, the results from which will be used to improve the representation of the evolution of aerosol optical properties in global chemical transport and climate models. In this report, we first summarize the general concept of aerosol processing by clouds, including the anticipated effects of cloud processing on specific aerosol optical properties. Next we describe the three field campaigns we undertook in order to investigate aerosol cloud processing. Finally, we present results from these field campaigns. Where appropriate we bring in the complementary measurements which allow this experiment to go beyond the measurement of cloud processing symptoms and actually diagnose the controlling factors in the system.

1.1 Cloud processing of aerosol particles

Clouds and aerosol particles can interact in several ways, including nucleation scavenging, coagulation, diffusion and washout. Clouds can also provide the interface for heterogeneous chemical reactions resulting in mass addition to scavenged particles (e.g., Kreidenweis et al., 2003) and multi-modal size distributions (e.g., Feingold and Kreidenweis, 2000). The relative dominance of each of these processes depend on both the characteristics of the cloud and the aerosol; however, Noone et al. (1992b) have shown that nucleation scavenging is likely to be the primary in-cloud mechanism for particle removal and will be the main focus here. Nucleation scavenging is the process whereby an aerosol particle grows into a cloud droplet in a supersaturated environment. The ability of an aerosol particle to act as a cloud condensation nucleus (CCN) depends largely on its size and on the fraction of water-soluble material in the particle. Nucleation scavenging is most effective for large soluble particles and less effective for

smaller or insoluble particles. When precipitation falls from the cloud, large soluble particles are preferentially removed from the system and the aerosol that remains when the cloud subsequently dissipates is enriched in smaller and insoluble particles. As described below, this enrichment has implications for the two optical properties controlling the radiative forcing efficiency of the aerosol, namely, the single-scattering albedo (SSA) and the backscatter fraction (BFR). SSA describes the relative contributions of scattering and absorption to light extinction, and BFR describes the amount of sunlight that is scattered back to space when the sun is directly overhead. Measurements on ambient aerosols typically yield SSA values around 0.9, with SSA as low as 0.4 for diesel soot and as high as 1.0 for pure sulfate aerosols. At visible wavelengths, BFR decreases from 0.5 for particles much smaller than the wavelength of light to nearly zero for particles much larger than the wavelength of light; measurements on ambient aerosols typically reveal backscatter fractions in the range 0.1-0.2. Based on the size and composition dependencies of nucleation scavenging and aerosol optical properties, we test the hypothesis that nucleation scavenging systematically reduces the single-scattering albedo and increases the backscatter fraction of the unscavenged aerosol. The results of these tests are described in section 3.

A main focus of cloud/aerosol research has been on how aerosols influence cloud properties, e.g., indirect effect (e.g., Charlson et al., 1987; Rosenfeld, 2000); here we explore how clouds influence the properties of aerosol particles. How clouds process aerosols is a function not only of the characteristics of the aerosol particles, but also of the cloud properties. Three cloud parameters which are important for aerosol processing are liquid water content, cloud drop size and updraft velocity. Kasper-Giebl et al. (2000) have measured different scavenging efficiencies

for sulfate and carbonaceous aerosol and noted that these scavenging efficiencies varied with cloud LWC. To the extent that coagulation and impaction processes control aerosol scavenging by cloud drops, cloud drop size is directly important for aerosol/cloud drop interactions, although Noone et al., (1992b) suggest these processes are not particularly important. Cloud drop size also plays a role in cloud lifetime (being a determining factor for when precipitation starts). Updraft velocity controls the supersaturation reached in the cloud which in turn determines which particles are activated (i.e., scavenged by in-cloud nucleation). Feingold and Kreidenweis (2000) have shown that lower updraft velocities can result in more nucleation scavenging during aerosol cycling through clouds.

1.2 Aerosol scattering, back-scattering and backscatter fraction

Aerosol total scattering (i.e., the sum of forward and backward scattering) gives an indication of how much aerosol is present. Observed total scattering values range from less than 10 Mm^{-1} in clean environments to a factor of 40 or more higher in polluted or dusty environments. The amount of scattering varies not only as a function of location but can also vary significantly at the same location depending on sources, transport and meteorology (e.g., Delene and Ogren, 2002). Back-scattering (light scattered in the direction of the light source) is, like total scattering, related to the amount of aerosol present; however, back-scattering is also a strong function of particle size. The ratio of total scattering to back-scattering, the 'backscatter fraction (BFR)' is thus primarily an indicator of particle size, with higher values suggesting the presence of smaller particles. BFR is one integral property of the angular distribution of light scattered by aerosols, also called the phase function, used in modeling the impact of aerosols on radiative fluxes and climate. Another common parameterization of the phase function in radiative forcing

calculations is the asymmetry parameter. The BFR can be related to asymmetry parameter using the methodology of Marshall et al. (1995).

Delene and Ogren (2002) have shown that the BFR varies systematically with amount of total light scattering - it tends to be higher for clean conditions and lower for high aerosol loadings (Figure 1a). One possible explanation for this observation is that cloud processing preferentially scavenges and removes larger particles, resulting in cleaner conditions with a post-cloud aerosol size distribution shifted towards smaller particles. Conditions characterized by higher aerosol concentrations that have not undergone cloud processing retain a broader aerosol size distribution including larger particles. Noone et al. (1992) showed that, in a polluted cloud, in-cloud scavenging preferentially removes larger particles while particles smaller than 0.3 μm remain as interstitial aerosol. Hallberg et al. (1994) also noted preferential scavenging of larger particles, although they found that interpretation of their results were complicated by possible influences of aerosol composition/mixture state and entrainment of drier air into the cloud. Results like this are consistent with observations of Delene and Ogren (2002).

1.3 Aerosol absorption and single scattering albedo

While particles that are primarily light scattering have been studied extensively, the influence of light absorbing particles in the atmosphere is still not well understood. Elemental carbon (EC) particles, a component of soot, are the primary particulate absorbers of solar radiation in the atmosphere. EC particles are typically generated by combustion and can be natural (e.g., biomass burning) or anthropogenic (e.g., diesel soot) in origin. According to the IPCC report (2001), combustion aerosol and mineral dust are the main components contributing to the

uncertainty in estimates of direct aerosol forcing. Regardless of the source of light absorbing particles in the atmosphere, a better understanding of their lifetime and processing in the atmosphere will improve our ability to model the aerosol SSA, increasing accuracy in climate forcing calculations. Haywood and Shine (1996) have shown that the sign of the radiative forcing due to aerosols depends on SSA. Here we address one aspect of the EC lifecycle in the atmosphere: cloud processing of EC-containing aerosol.

Differential cloud scavenging as a function of aerosol hygroscopicity may result in changes in the relative amount of absorption to scattering in the unscavenged aerosol (Ogren and Charlson, 1983) and may be one cause of the systematic dependence of SSA on loading (Figure 1b) observed by Delene and Ogren (2002). Figure 2 illustrates the two extreme conditions for EC/cloud interactions. Figure 2a shows the case where the EC (e.g., soot) is hydrophobic and unlikely to act as CCN or to coagulate with cloud drops (e.g., Noone et al., 1992a). The EC may remain after other particles are removed by nucleation scavenging, resulting in a relatively blacker interstitial and post-cloud aerosol. In Figure 2b "aged" EC can become coated with other species such as sulfates or soluble organics (through condensation and/or coagulation processes) making the composite soot particles larger and more hygroscopic and thus more likely to become incorporated into cloud or fog droplets. Conversion of soot aerosols from hydrophobic to hygroscopic particles is the rate limiting step in this mechanism (e.g., Ogren and Charleson, 1983; Cooke and Wilson, 1996). There is a competition between the conversion rate to a hygroscopic particle and onset of precipitation. If precipitation removes water-soluble substances that could coagulate with or condense upon EC before the EC has acquired a hygroscopic coating, then the conversion of EC to a hygroscopic form will take much longer.

Both experimental and modeling studies support the notion of competition between particle conversion rates and onset of precipitation. Noone et al. (1992a) noted that EC particles remained primarily in the interstitial aerosol during a fog experiment in Italy. In a mountain cloud experiment, Hallberg et al. (1994) investigated whether chemical composition, specifically EC and sulfate species, influenced the partitioning of particles between cloud drops and interstitial air. They found that sulfate-containing particles were scavenged by cloud droplets three times more efficiently than EC, although they were unable to determine whether this difference was due solely to chemical composition or to differences in the size distribution of the two aerosol species. In a different study in a more remote location, Gieray et al. (1997) found that sulfate and soot aerosol had similar scavenging fractions, although sulfate aerosol was still scavenged slightly more efficiently than soot. More recently, Laj et al. (2001) found that EC particles tended to remain as interstitial aerosol in ice clouds; and Ogren et al. (2004) showed a strong correlation between decreases in SSA and presence of cloud. Modeling work by Chung and Seinfeld (2002) is consistent with these in situ observations. They compared measurements of carbonaceous aerosol with values predicted using a global circulation model with tracer transport capabilities. The model consistently under-predicted carbonaceous aerosol concentrations. The authors suggest that one source of the underestimation could be the model parameterization of wet scavenging (i.e., the model may over-estimate the potential of clouds to scavenge EC).

The uncertainties in EC scavenging reported in the literature may be due to the fact that the characteristics of EC particles can change during their lifetime in the atmosphere. Condensation

of soluble materials on the surface of EC particles and/or coagulation with soluble particles can increase the hygroscopicity of the EC-containing particles. Gieray et al. (1997) and references therein, note the increasing fraction of EC scavenged by clouds with increasing distance from the aerosol source. Alternatively, condensation of hydrophobic film forming compounds on aerosol particles may reduce the number of cloud drops activated (i.e., the number of aerosol particles scavenged by nucleation) (Feingold and Chuang, 2002a). Optical measurements alone will not provide information about chemical characteristics of the EC, but will provide one piece of the puzzle.

1.3 Hypotheses

Cloud processing affects aerosol chemical and microphysical properties. The observed changes depend on the initial or pre-cloud nature of the particles (i.e., mixing state, composition, size distribution, etc.) as well as the nature of the cloud (e.g., liquid water content). It follows that aerosol optical properties will also be affected by cloud processing. Below we list several hypotheses describing the influence of clouds on aerosol optical properties:

1. BFR will increase in cloud scavenged air and interstitial aerosol.
2. SSA will decrease in cloud-scavenged air and interstitial aerosol.
3. Distinct aerosol types will interact differently with clouds, but the general trends will likely be the same. For example, SSA will decrease for all aerosol types but the decrease will be less if the absorbing aerosols have aged and are internally mixed with soluble aerosols.
4. The radiative properties of cloud-processed aerosol are quite different than pre-cloud aerosol.

Table 1 summarizes the measurements and calculations needed to test these hypotheses. We describe the results from testing these hypotheses and document how aerosol optical properties change with cloud processing in the Results section (section 3).

2.0 Field Campaigns and Instrumentation

A series of three field experiments (see Table 2) were performed to determine the effect of cloud/fog processing on the optical properties of several types of aerosols. The aerosol studied in these field campaigns included clean marine (Point Reyes, CA), highly absorbing, urban-influenced (near Manchester, UK) and less absorbing, urban-influenced (near Oklahoma City). The clean marine aerosol had a fairly broad size distribution so changes in particle size due to cloud processing would be easy to see. The urban-influenced aerosol provided a good opportunity to look at changes in SSA due to cloud processing. Below we briefly describe each of the measurement locations and then summarize the basic measurements made for each campaign.

2.1 Measurement Locations

Over the course of the project we participated in a series of month-long field intensives that that permitted us to measure the optical properties of different types of aerosols and to determine the changes resulting from the cloud/aerosol interactions. For the surface studies, we chose sites and time periods where the climatological prevalence of clouds/fog were relatively high, while for the aircraft studies climatology suggested that we would be able to find appropriate clouds to sample the aerosols before, during and after cloud processing.

2.1.1 Point Reyes, CA

In early 2005, the opportunity arose to co-locate a CVI system in July 2005 in tandem with the standard aerosol observing system (AOS) that was to be deployed with the ARM mobile facility (AMF) during a planned six-month field campaign in Point Reyes National Seashore in California (38.00 N 123.03 W, 10 m asl). This deployment took part in conjunction with the MArine Stratus Radiation Aerosol and Drizzle (MASRAD) study (http://www.db.arm.gov/cgi-bin/IOP2/selectExecSummary.pl?iopName=amf2005masradiop&person_id=). Point Reyes has been called one of the foggiest places on earth, and while that may be hyperbole, the foggy nature of the locale provided an excellent opportunity to study the inter-relationship between aerosol particle and cloud droplet properties using a surface-based observing platform. In addition to the cloud/aerosol research, several other complementary aerosol projects also took place at the site including (a) an intercomparison of the Cadenza cavity ring down technique (funded by NASA) and PSAP for measuring light absorption (b) coordinated ultrafine and chemistry aerosol particle measurements and (c) measurement of aerosol optical, physical and chemical properties during cloud free conditions at a marine site.

The advantages of such a deployment were myriad. Point Reyes was a relatively easy location to access. The infrastructure and technical support provided by ARM were excellent and no usage fees were charged. The location and support at the AMF simplified the participation of all the ASP participants (Ogren, Berkowitz, Laskin). Because the AMF AOS system was already in place and set-up to sample sub-5 micrometer aerosol (i.e., interstitial aerosol during foggy conditions), we just had to provide the one set of the aerosol instruments needed to measure aerosol properties downstream of the CVI inlet.

2.1.2 Holme Moss, UK

One scientific disappointment in the Point Reyes campaign was how clean the air was - air masses during the month-long study came primarily from the North Pacific and contained little or no elemental or organic carbon, two constituents of interest. For our second field experiment we looked for somewhere foggy and polluted. Holme Moss (53.53°N 1.86°W 525 m asl) (http://cloudbase.phy.umist.ac.uk/field/) has been used as a research site by the University of Manchester for more than a decade for both field campaigns and long term climatological measurements (e.g., Beswick et al., 2003). The site is located approximately 30 km to the north and east of the city of Manchester on top of Black Hill. Long-term climatology suggested that the site would frequently be in cloud (150-200 hrs/month in autumn), and the site was indeed in fog ~22% of the sampling period (fog defined here for simplicity as visibility < 5km). While the site had potential to receive fresh pollution from either Manchester or Leeds, depending on which way the wind was blowing, during the campaign the wind was primarily from the southwest meaning Manchester was the main source of aerosol sampled.

For the deployment, a trailer was rented for the instrumentation brought by NOAA and for some of the University of Manchester (UM) measurements. UM also brought up their seatainer which housed the vast majority of their in-situ instruments. A tall scaffolding was erected for mounting the ambient/interstitial aerosol (AIA) inlet and the CVI inlet. A second scaffolding structure was used for various cloud microphysical and meteorological instruments operated by UM.

The measurements at Holme Moss took place during the month of November, 2006. Site preparation (e.g., scaffolding, trailer installation, etc.), instrument set-up, and testing took about 10 days so measurements began on November 6, 2006 and continued through December 4, 2006. UM provided invaluable logistical support working with customs agents, transporting equipment from the University to the site and most of all in getting the site prepared.

2.1.3 Oklahoma City, OK

The final field experiment we performed occurred as part of the Cumulus Humilis Aerosol Processing Study (CHAPS) campaign in Oklahoma in June 2007. The stated goal of the CHAPS campaign was to "study interactions of aerosols on clouds and of clouds on aerosols" with particular interest in how emissions from a mid-sized city affected these interactions. Thus it meshed nicely with the hypotheses we wished to explore. The major difference in this campaign compared to the two previous experiments was that in this case the platform was the ASP G1 aircraft managed by Battelle. The aircraft platform enabled us to seek the clouds rather than waiting for the clouds to come to us. A study of cloud chord length (pers. comm., L. Berg, 2006) based on climatological measurements made at DOE's Southern Great Plains facility suggested that the cumulus humilis clouds would be frequent enough and sizeable enough for the proposed investigations on aerosol-cloud interaction.

The G1 aircraft was based in Ponca City, OK. From there the plane would fly various flight patterns determined based on meteorology, in-flight observations and mission goals. The G1 flew 12 missions over the course of the month. The most common flight pattern was a series of profiles (walls) upwind and downwind of Oklahoma City intended to sample clean (upwind) conditions and the urban plume (downwind). Each profile was designed to include an above-

cloud, below-cloud and two in-cloud legs. The two in-cloud legs were included so that the aerosol mass spectrometer (AMS) which measured non-refractory aerosol chemistry could spend one leg sampling interstitial aerosol from the iso-kinetic (ambient) inlet and one leg sampling cloud drop residuals through the CVI inlet. During the campaign the weather tended not to cooperate with the general goals of CHAPS – June 2007 was when Texas, Oklahoma and Kansas all had devastating floods. As one scientist noted the clouds tended to be more of the 'cumulus humongous' variety than of the cumulus humilis type. Nonetheless, based on in-flight observations and some preliminary data QC, the G1 successfully intercepted the Oklahoma City plume.

2.2 Basic measurements

Despite differences in the platforms, collaborators and instrumentation during each field campaign, the basic scheme for studying aerosol cloud interactions was quite similar. Each experiment involved a set of tandem inlets, one designed to sample ambient or interstitial aerosol (depending whether fog was present or not) and one (the CVI) designed to sample cloud drop residuals. Downstream of these inlets were some duplicate instrumentation and then some sort of switching system to allow non-duplicate instruments to switch between inlet systems in order sample both interstitial and cloud drop residuals when the inlets were in cloud. Table 2 lists the aerosol and ancillary instrumentation deployed at each field site. Figure 3 is a schematic of the instrument sampling set up at Point Reyes. It is representative of the system for the other two sites, although the instruments and inlet switching were slightly different for each experiment.

Our research focus is primarily on the aerosol optical properties (Table 2 includes some of the relevant instrumentation deployed by collaborators). The basic aerosol optical property measurements required to address our hypotheses are the partitioning of aerosol light absorption, total light scattering, and hemispheric backscattering between interstitial air and the cloud droplets. These measurements are the fundamental components needed to calculate aerosol radiative forcing. The specific aerosol optical property measurements we made during these field intensives to obtain the data for hypothesis testing are listed in Table 1. The directly measured quantities permit us to derive several key aerosol properties important in aerosol radiative forcing, including SSA and BFR. Measurements were conducted so that both the pre-cloud and in-cloud aerosol (i.e., aerosol incorporated into clouds droplets and interstitial aerosol particles) were sampled. Our in-cloud experimental approach was to sample simultaneously two size fractions of particles and droplets. Nucleation-scavenged particles grow rapidly above cloud base to diameters larger than a few micrometers, while the unscavenged particles remain in the size fraction below a few micrometers. At the surface a counterflow virtual impactor (CVI, Ogren et al., 1985; described below) was used to extract cloud droplets larger than ~8 μm diameter from the surrounding air, while the ambient/interstitial inlet only sampled particles less than ~5 μm diameter. An inertial impactor provided the cutsize for the interstitial aerosol. On the G1, the isokinetic inlet was efficient for diameters less than ~5 μm (e.g., low turbulence inlet (Wilson and Seebaugh, 2001)), while the cutsize of the airborne CVI was ~11 μm. For both the surface and airborne platforms there is an unavoidable size gap between the interstitial and cloud drop samples. Ideally, without the gap, the sum of these two size fractions would represent the total aerosol in the cloud allowing for closure. These complementary samples are subsequently dried to the same relative humidity (ca. 40%), and the optical properties of the dried particles are

measured with duplicate sets of instrumentation (Figure 3). A similar system was used in the Po Valley experiment in 1989 (Heintzenberg, 1992) and more recently at Åre, Sweden in the summer of 2003 (Ogren et al., 2004).

In addition to aerosol optical properties, the total particle number, N_{tot}, (measured using a CN counter) was measured downstream of both the aerosol and CVI inlets. Measurement of N_{tot} provides a sanity check on the measurements. Because the sum of interstitial particle number and cloud droplet number should be N_{tot} (in an ideal sampling system) we have a constraint to help us identify sampling problems. For example, on the airplane during in-cloud legs, drop shattering in the isokinetic inlet resulted in the interstitial particle number being significantly higher than the ambient particle concentration. Additionally, measurement of N_{tot} can help in determining whether the airmass is changing over the course of the cloud event (e.g., Noone et al., 1992b).

2.3 The CVI inlet

The counterflow virtual impactor was conceived by one the PIs (Ogren) in the early 1980s (Ogren et al., 1985). Its original application was aircraft-based sampling of Arctic clouds during the Marginal Ice Zone experiment (MIZEX-84). This airborne deployment was followed two years later by surface-based experiments which included characterization of the aerosol particles that result from evaporation of cloud droplets (Noone et al., 1988) and size dependent chemistry of cloud droplets (Ogren et al., 1989). In the last several decades, many researchers have found the CVI to be a useful technique for cloud/aerosol studies. A comprehensive list of CVI references is at http://www.esrl.noaa.gov/gmd/aero/pubs/cvi.html. Some examples include:

studies of the composition of ice nuclei (e.g., Christensson et al., 2000), studies of ship (e.g., Noone et al., (2000) and aircraft exhaust (e.g., Twohy and Gandrud, 1998). Ogren et al. (2004) utilized a ground-based CVI to investigate differences in interstitial versus cloud-scavenged SSA at a mountain top site in Sweden.

3.0 Results

Our hypotheses focused on characterizing the changes in aerosol optical properties associated with cloud/fog processing. Thus, our major goal was to use observational studies to determine the ranges of the cloud-induced changes to the aerosol optical properties for different types of aerosols. We present results for each of our hypotheses below. There are many other changes to the aerosol which can occur with atmospheric cloud/fog processing (e.g., chemical reactions); while the investigation of these changes was beyond the scope of our specific project, complementary measurements made by collaborators during the campaigns allow us to begin to investigate some of the mechanisms responsible for the observed changes. We present some of these results as well.

3.1 BFR will increase in cloud scavenged air and interstitial aerosol

Figure 4 shows differences in BFR for ambient and interstitial air for four sites at which we have made these types of measurements. The figure shows results from Point Reyes and Holme Moss as well as two other sites. (Mount Areskutan was a field site in Sweden, the aerosol could be categorized as remote continental; Chebogue Point measurements were made on the southwest coast of Nova Scotia and the aerosol was primarily aged urban plume from the east coast of the US). The Oklahoma G1 data is not included in these plots as data analysis is not complete at this

time. Also, as mentioned previously, we know that droplet shattering caused issues with the measurement of interstitial aerosol when sampling from the G1. Figure 4 shows that for all four types of aerosol, BFR increased for interstitial aerosol compared to that measured for cloud free aerosol. This is consistent with our hypothesis and suggests that the clouds are preferentially scavenging the larger aerosol, leaving smaller particles in the interstitial air.

3.2 SSA will decrease in cloud-scavenged air and interstitial aerosol

Figure 5 shows differences in SSA for ambient and interstitial air for the same four sites. Again a consistent picture emerges – the SSA is lower in the interstitial air than it is for the cloud free air. Thus, as we hypothesized, the clouds appear to be less likely to incorporate absorbing aerosol than scattering aerosol resulting in darker aerosol in the interstitial air.

3.3 Distinct aerosol types will interact differently with clouds, but the trends will be the same

Table 3 summarizes the observed changes in BFR and SSA as a function of aerosol type for the four sites shown in figures 4 and 5. While the trends are the same for each site, the magnitude of the change between clear and cloudy air can differ significantly – for example at Point Reyes the decrease in single scattering albedo is very small compared to the decrease observed at Holme Moss. Table 3 shows that the magnitude of the change can be quite different. Explaining these differences in magnitude requires complementary measurements such as aerosol size distribution and chemistry.

3.4 Radiative properties of cloud-processed aerosol are different than pre-cloud aerosol

Figure 6 shows aerosol radiative forcing efficiency (RFE) at the top of the atmosphere calculated based on the formulation of Haywood and Shine (1995) for the four sites. For this calculation the only variables are BFR and SSA – for aerosol comparison purposes everything else (zenith angle, surface albedo, etc) are assumed to be identical for all sites. The aerosol RFE for most of the sites is quite similar, -25 to -30 W m^{-2}, with Holme Moss being an outlier having a median RFE of -16 W m^{-2} for clear sky aerosol. The Holme Moss RFE tends to be more positive (i.e., warming) because it is a more absorbing aerosol. As seen in figure 5, for a given location and aerosol type, cloud processed aerosol also tends to be more absorbing (lower SSA) than the aerosol measured during cloud-free conditions. The lower SSA values are the primary explanation for the reduction in cooling (increased RFE) observed for interstitial aerosol. Point Reyes is the exception to this observation and actually shows a slight decrease in RFE for interstitial aerosol. This can be explained by noting that the fog-induced changes in BFR and SSA have opposite effects on RFE. At Point Reyes the change in BFR causes a decrease in RFE which is not counteracted by the relatively small change in SSA.

3.5 Complementary Measurements

Cloud-aerosol interactions are a function of both cloud properties (e.g., phase, liquid water content) and aerosol properties (e.g., size, composition, morphology, etc.), and the range of aerosols and clouds that were sampled during these three field campaigns provide an excellent basis to start developing parameterizations for chemical transport models describing the effects of cloud scavenging on aerosol climate-forcing properties. In addition, by relating the particle microphysics and chemistry to the particle hygroscopic and optical behavior it is possible to

elucidate some of the mechanisms and factors influencing direct and indirect aerosol radiative forcing in the ambient (humid!) atmosphere.

Quinn et al (2005) presents an elegant example of how combined chemical and optical aerosol measurements can be used to develop useful parameterizations for modelers. They show how a measure of the chemical nature of the aerosol - the relative amount of sulfate and organic carbon - is well-correlated with the measured dependence of light scattering on relative humidity (f(RH)), and suggested a simple parameterization for predicting f(RH) in chemical transport models. We can augment the analysis of Quinn et al (2005) by combining our measurements of f(RH) at Point Reyes and Holme Moss with the aerosol mass spectrometer measurements made by PNNL and UM respectively. Figure 7 shows how the Holme Moss f(RH) aerosol fits into the Quinn et al. parameterization scheme.

Specifically complementary measurements help answer the following questions: What are the microphysical and chemical properties that distinguish interstitial particles from those that are cloud scavenged? How does the CCN concentration vary with dry aerosol composition and size distribution? What are the processes controlling aerosol/cloud interactions?

We have begun the analysis to address some of these questions. Figure 8 shows the activated fraction (CCN/CN) measured at Holme Moss as a function of two indicators of aerosol composition. Figure 7a shows that CCN activity increases as SSA increases. This is consistent with the common assumption that absorbing aerosol tends to be hygrophobic. Figure 7b shows that CCN activity decreases as relative amount of organic carbon in the aerosol increases. This

is consistent with the idea presented in Quinn et al. (2005) showing that hygroscopic growth at sub-saturated conditions is less for aerosol for a high organic aerosol.

A cloud parcel model (e.g., Feingold and Kreidenweis, 2000) in combination with a particle scattering model is necessary to interpret the results from these complementary measurements. The model would need to include parameterizations of aerosol microphysical and chemical properties, cloud droplet activation and the aerosol optical properties. The model would relate the information on the particle chemical composition and size to the aerosol particles that become cloud condensation nuclei (CCN). The particle scattering model would connect the results on aerosol size, composition and hygroscopic growth to the optical properties of the cloud-scavenged and interstitial aerosol. This information on aerosol cloud partitioning and its effect on aerosol optical and cloud properties could then be applied to regional climate forcing models.

4.0 Conclusions

The ASP aims to improve predictive climate modeling through improved understanding of the aerosol radiative forcing of the climate. Here we have addressed one of the uncertainties in the distribution and fate of aerosols (i.e., cloud processing) and explored how it relates to changes in aerosol optical properties and radiative fluxes for multiple aerosol types. Based on the results from the three field campaigns described above, we have been able to assess our general hypotheses. We found that clouds tend to scavenge larger, less scattering aerosol leaving the

darker, smaller aerosol in the interstitial air. In terms of intrinsic aerosol properties this means that BFR increases and SSA decreases in cloud scavenged air and interstitial aerosol. As BFR and SSA are both important factors in aerosol radiative forcing it follows and we showed here that the radiative properties of the cloud-processed aerosol are quite different than the pre-cloud aerosol. We observed cloud processing of aerosol for multiple aerosol types and while the magnitude of the changes differ as a function of aerosol type the general trends are the same.

Complementary measurements made by our collaborators, e.g., aerosol chemistry, is already allowing us to explore how particle composition influences water/aerosol interactions with implications for both direct and indirect forcing. As we work together with this large data set some other ideas we hope to explore are:

1) improved parameterization of EC processing by clouds

2) better understanding of size and composition dependent aerosol processing by clouds

3) reduced uncertainty in EC cycle and lifetime in atmosphere

4) better understanding of the cloud processing mechanisms affecting aerosol properties

Incorporation of findings from these planned explorations into climate models will reduce the uncertainty in predictive modeling capabilities and improve our ability to identify the amount of aerosol radiative forcing versus other forcing factors such as greenhouse gases.

Table 1 Optical measurements and derived aerosol optical properties

	Measured properties	**Instrument providing measurement**
σ_{sp}	Total aerosol light scattering at three wavelengths (450, 550, 700 nm) at low (<40%) relative humidity	Integrating nephelometer
σ_{ap}	Aerosol light absorption at three wavelengths (~450, ~550, ~700 nm) at low (<40%) relative humidity	Particle soot absorption photometer (PSAP)
σ_{bsp}	Hemispheric back-scattering at three wavelengths (450, 550, 700 nm) at low (<40%) relative humidity	Integrating nephelometer
	Derived properties	
SSA	The aerosol single-scattering albedo, defined as $\sigma_{sp}/(\sigma_{ap} + \sigma_{sp})$, describes the relative contributions of scattering and absorption to the total light extinction. Purely scattering aerosols (e.g., sulfuric acid) have values of 1, while very strong absorbers (e.g., elemental carbon) have values around 0.3.	Need nephelometer + PSAP measurements
BFR	Radiative transfer models commonly require one of two integral properties of the angular distribution of scattered light (phase function): the asymmetry factor *g* or the hemispheric backscatter fraction BFR. The hemispheric backscatter fraction BFR is defined as σ_{bsp}/σ_{sp}. The asymmetry factor is the cosine-weighted average of the phase function, ranging from a value of -1 for entirely backscattered light to +1 for entirely forward-scattered light and can be estimated using BFR (Marshall et al., 1995)	Need nephelometer measurements

Table 2 Relevant instrumentation for each experiment

Field Site	Instruments	Measured property	Instrument Mentor(s)
Point Reyes CA	TSI Nephelometer [1,2]	Spectral σ_{sp}, σ_{bsp}	NOAA
	Radiance Research PSAP[1,2]	Spectral σ_{ap}	NOAA
	TSI CNC[1,2]	Number concentration, N_{tot}	NOAA
	DMT CCN[1,5]	CCN number concentration	NOAA and PNNL
	Humidograph[1,5]	σsp as function of RH (f(RH))	NOAA
	Tunable diode laser hygrometer[1,4]	Water vapor mixing ratio	NOAA
	Aerodyne Aerosol Mass Spectrometer[3]	Non-refractory aerosol chemistry	PNNL
	Time resolved aerosol collector (TRAC) [2]	Elemental aerosol composition	PNNL
	Scanning mobility particle sizer[5]	Aerosol size distribution	PNNL and BNL
	Vaisala Present Weather Sensor	Visibility and precipitation type	ARM/NOAA
	Meteorology	Temperature, RH, pressure, winds	ARM
Holme Moss UK	TSI Nephelometer [1,2]	Spectral σ_{sp}, σ_{bsp}	NOAA
	Radiance Research PSAP[1,2]	Spectral σ_{ap}	NOAA
	TSI CNC[1,2]	Number concentration	NOAA
	DMT CCN[1,2,3]	CCN number concentration	NOAA and UM
	Humidograph[1,5]	σsp as function of RH (f(RH))	NOAA
	Tunable diode laser hygrometer[1,4]	Water vapor mixing ratio	NOAA
	DMT Single particle soot photometer[3]	Soot fraction and coating thickness	UM
	Aerodyne Aerosol Mass Spectrometer[3]	Non-refractory aerosol chemistry	UM
	Scanning mobility particle sizer[3]	Aerosol size distribution	UM
	Vaisala Present Weather Sensor	Visibility and precipitation type	UM
	PMS Forward scattering spectrometer probe	Cloud drop number and size	UM
	Gerber Particle volume monitor	Cloud LWC, drop effective radius	UM
	Meteorology	Temperature, RH, pressure, winds	UM
Oklahoma G1 aircraft	TSI Nephelometer [1,2]	Spectral σ_{sp}, σ_{bsp}	NOAA
	Radiance Research PSAP[1,2]	Spectral σ_{ap}	NOAA
	TSI CNC[1,2]	Number concentration	NOAA
	Particle absorption photo-acoustic cell[2]	σap	LANL
	DMT CCN[5]	CCN number concentration	PNNL
	Tunable diode laser hygrometer[1,4]	Water vapor mixing ratio	NOAA
	Aerodyne Aerosol Mass Spectrometer[3]	Non-refractory aerosol chemistry	PNNL/BNL
	Time resolved aerosol collector (TRAC) [2]	Elemental aerosol composition	PNNL
	Scanning mobility particle sizer[5]	Aerosol size distribution	BNL
	PMS Forward scattering spectrometer probe	Cloud drop number and size	BNL
	Meteorology	Temperature, RH, pressure, winds	PNNL
	Aircraft parameters	Speed, location, pitch, yaw, etc.	PNNL

[1]Mentored by NOAA as part of our research
[2]Duplicate instrument (i.e., one for each inlet)
[3]Downstream of a switch, enabling switching between CVI and AIA inlet
[4]CVI inlet only
[5]AIA inlet only
Note: As part of ASP infrastructure PNNL provided one basic aerosol optics system (nephelometer, PSAP, CNC) for Point Reyes and duplicate aerosol optics systems for Holme Moss and Oklahoma (counting the G1 instruments as part of ASP infrastructure)

Table 3 Trends in aerosol properties due to cloud processing

Site, aerosol type	**%Change BFR[1]**	**%Change SSA[1]**	**%Change RFE[1]**
Mt. Areskutan, Remote continental	-20.14	5.73	-7.41
Chebogue Point, Aged urban	-2.26	2.64	-10.34
Point Reyes, Clean marine	-17.43	1.11	3.57
Holme Moss, Aged urban/biomass burning	-19.05	9.88	-31.25

[1]%Change property = $(\text{property}_{\text{ambient}} - \text{property}_{\text{in-cloud}})/\text{property}_{\text{ambient}}$

Figure 1 Systematic variation of (a) aerosol back-scattering fraction and (b) single scattering albedo with light scattering (after Delene and Ogren, 2002). BND = Bondville, IL; SGP =, Lamont, OK (ARM-CART site); WSA=Sable Island, Canada; NSA= Barrow, AK (ARM site).

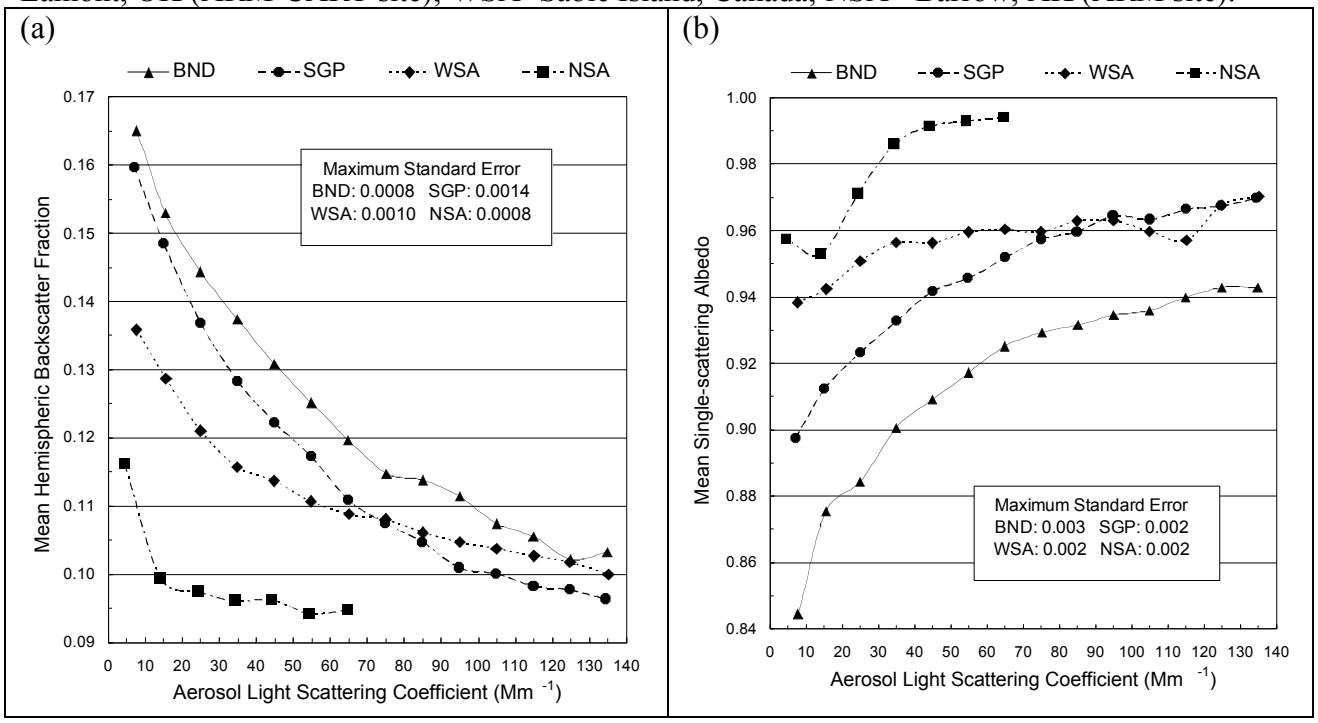

Figure 2 Exaggerated schematic of difference in processing for uncoated and coated EC particles.

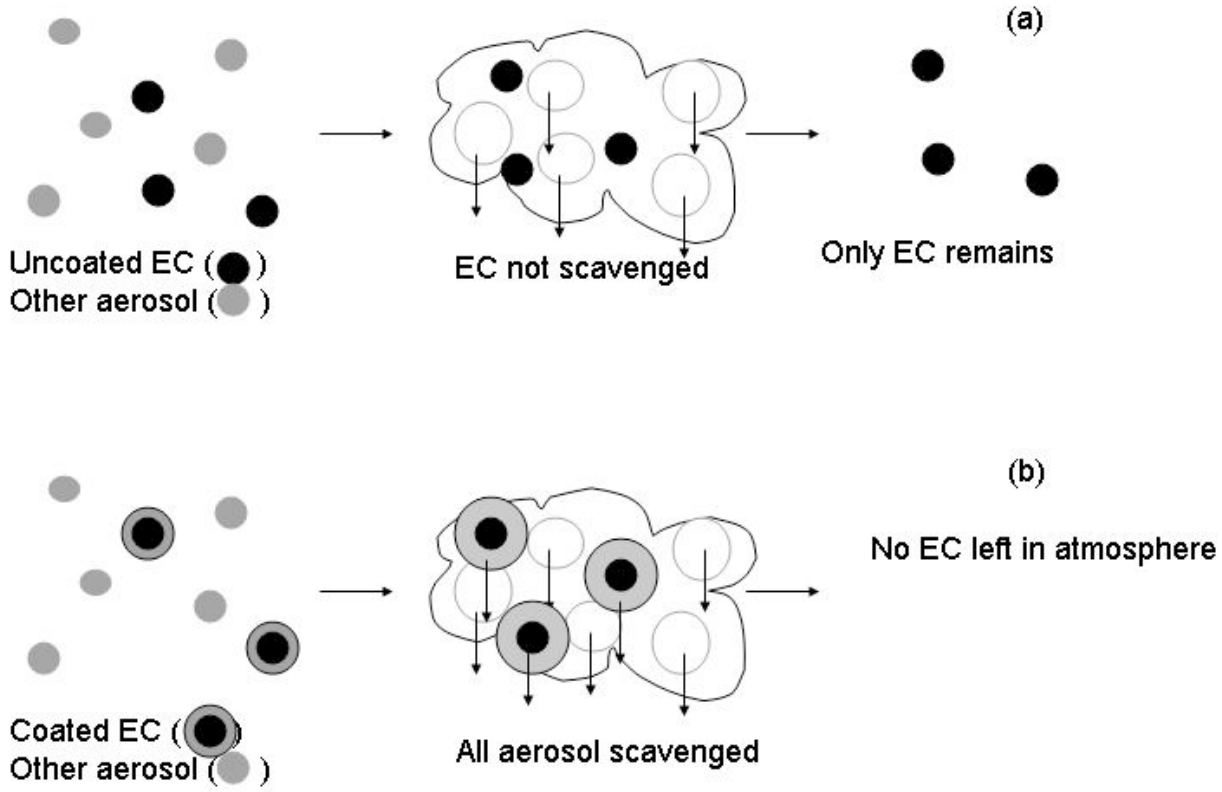

Figure 3 Schematic of Point Reyes sampling system (shows AMS sampling from AIA inlet)

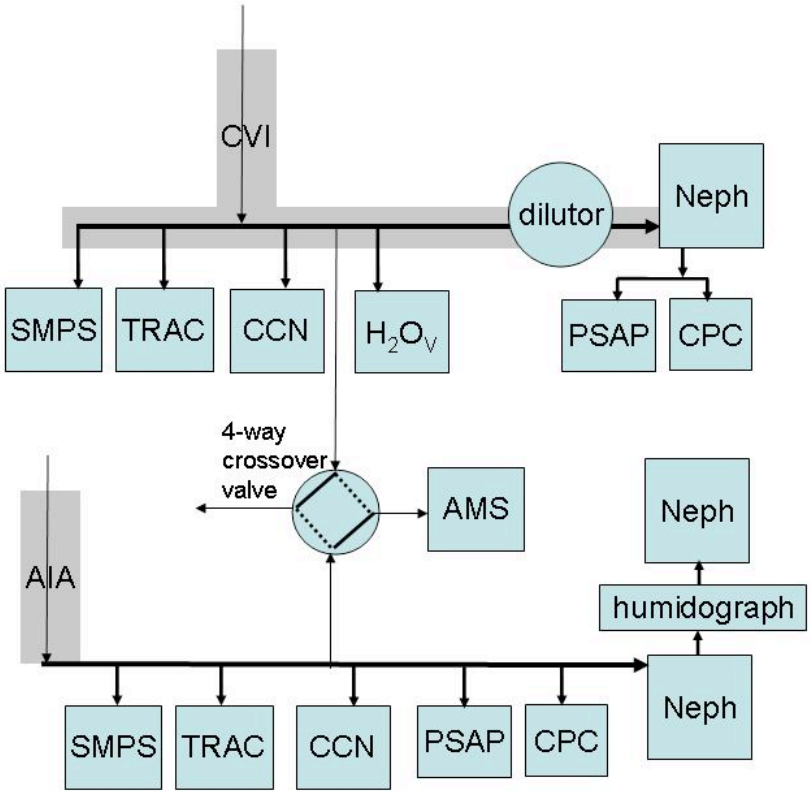

Figure 4 BFR for ambient and interstitial aerosol. These are box-whisker plots, with the line in the center of the box representing the median value, the top and bottom of the box are the 25th and 75th percentile and the ends of the whiskers are the 5th and 95th percentile.

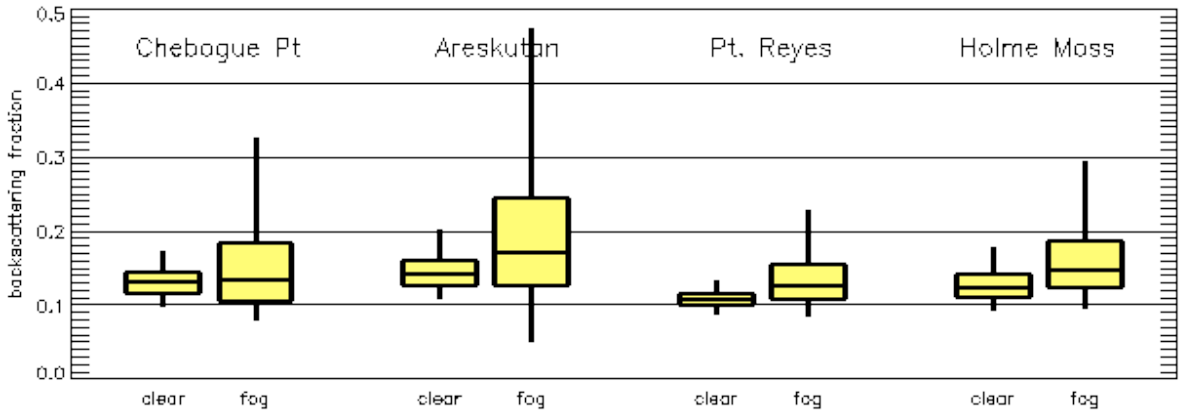

Figure 5 SSA for ambient and interstitial aerosol

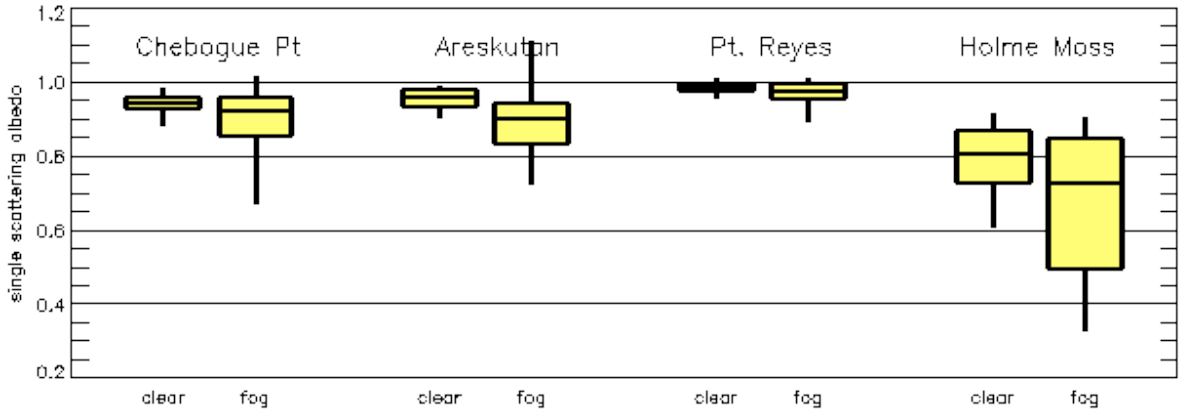

Figure 6 RFE for ambient and interstitial aerosol

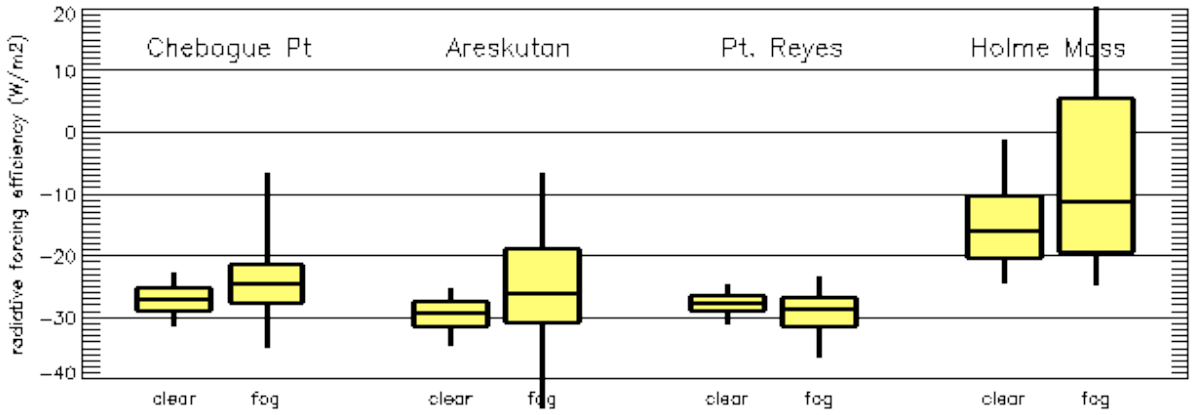

Figure 7 Parameterization of aerosol hygroscopicity as a function of aerosol composition (details in and figure from Quinn et al., (2005)); Holme Moss line added for this report.

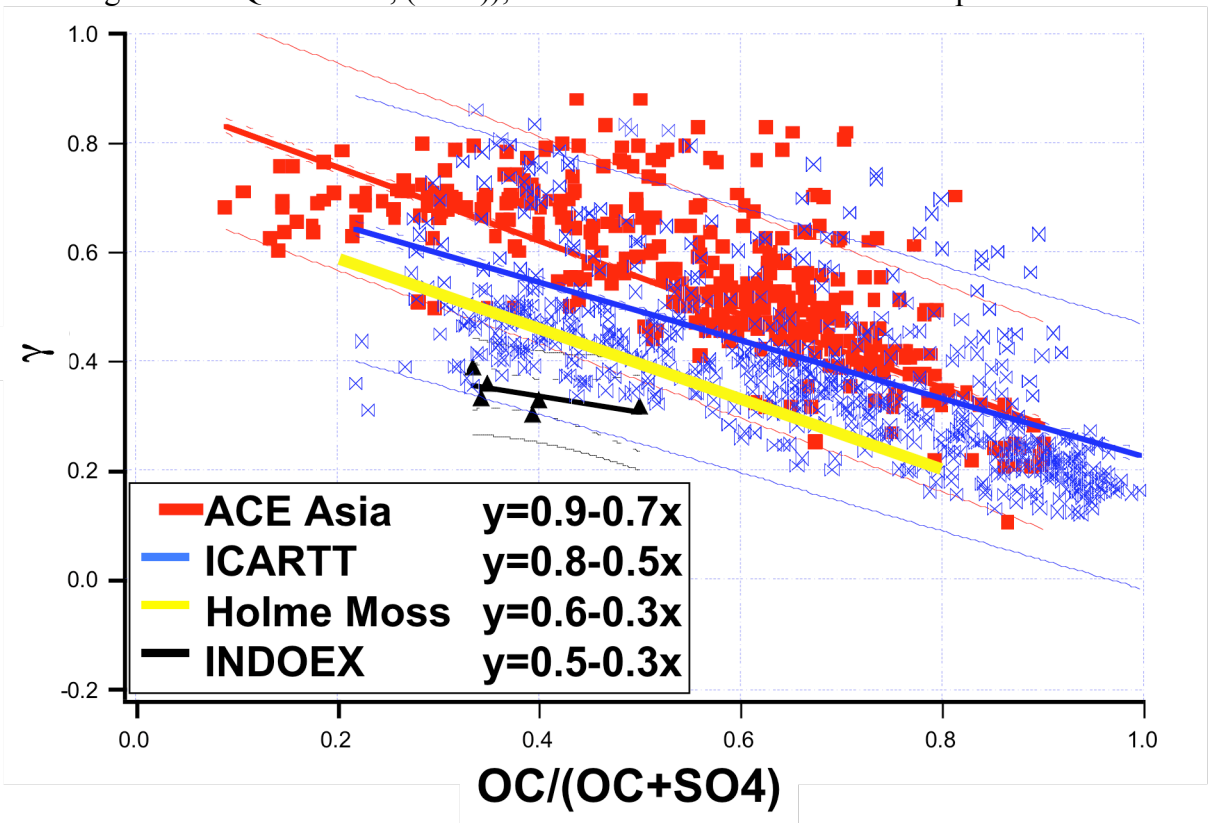

Figure 8 Activated fraction as a function of (a) single scattering albedo and (b) ratio of organic carbon mass to mass of organic carbon and sulfate (OC/(OC+SO4)) derived from AMS.

(a)

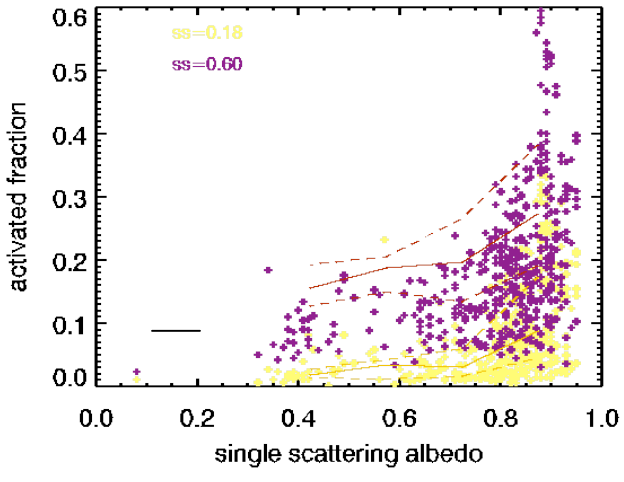

(b)

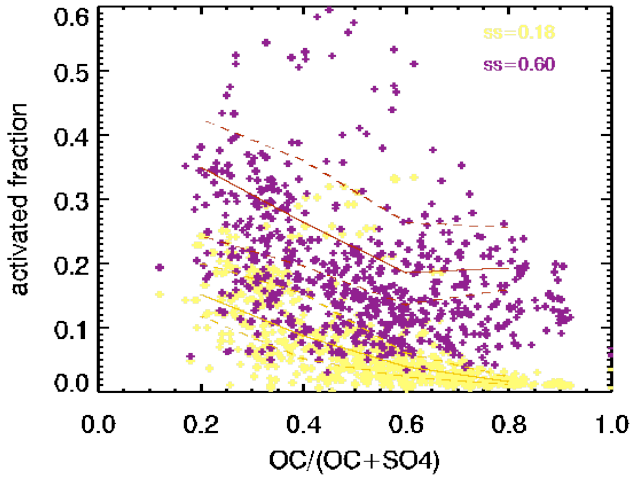

References

Beswick KM, Choularton TW, Inglis DWF, Dore AJ, Fowler D, "Influences on long-term trends in ion concentration and deposition at Holme Moss," *Atmos. Environ*., 37, 1927-1940, 2003.

Charlson, R.J., Lovelock, J.E., Andreae, M.O, Warren, S.G., "Oceanic phytoplankton, atmospheric sulfur, cloud albedo and climate," *Nature*, 326, 655-661, 1987

Christensson, A., J.-F. Gayet, et al "In situ observations of a reduction in effective crystal diameter in cirrus clouds near flight corridors." *Geophys. Res. Lett.,* 27, 681-684, (2000).

Chung, S.H. and J.H. Seinfeld, "Global distribution and climate forcing of carbonaceous aerosols," J. Geophys. Res., 107, D19, 4407, doi:10.1029/2001JD001397, 2002.

Cooke, W.F., and J.J.N. Wilson, "A global black carbon aerosol model," *J. Geophys. Res*., 101 (D14), 19395-19409, 1996.

Delene D.J. and J.A. Ogren, "Variability of aerosol optical properties at four North American surface monitoring sites," *J. Atmos. Sci.,* 59 (6): 1135-1150, 2002.

Feingold, G. and P.Y. Chuang, "Analysis of the influence of film-forming compounds on droplet growth: Implications for cloud microphysical processes and climate," *J. Atmos. Sci.,* 59 (12), 2006-2018, 2002.

Feingold, G., and S. Kreidenweis, "Does cloud processing of aerosol enhance droplet concentrations?," *J. Geophys, Res.*, 105 (D19), 24351-24361, 2000.

Gieray, R., P. Wieser, T. Engelhardt, E. Swietlicki, H.-C. Hansson, B. Mentes, D. Orsini, B. Martinsson, B. Svenningsson, K.J. Noone, J. Heintzenberg, "Phase partitioning of aerosol constituents in cloud based on sing-particle and bulk analysis, *Atmos. Environ.,* 31, 2491-2502, 1997.

Hallberg A., J.A. Ogren, K.J. Noone, J. Heintzenberg, A. Berner, I. Solly, C. Kruisz, G. Reischl, S. Fuzzi, M.C. Facchini, H.C. Hansson, A. Wiedensohler and I.B. Svenningsson, Phase partitioning for different aerosol species in fog, *Tellus* (B) 44, 545-555, 1992.

Hallberg, A., Ogren, J.A., Noone, K.J., Okada, K., Heingzenberg, J., and Svenningsson, I.B. "The influence of aerosol particle composition on cloud droplet formation," *J. Atmos. Chem* 19, 153-171, 1994.

Haywood, J.M., and K.P. Shine, "The effect of anthropogenic sulfate and soot aerosol on the clear sky planetary radiation budget," *Geophys. Res. Lett.*, 22 (5), 603-606, 1995.

Heintzenberg, J., "The Po Valley Fog Experiment 1989. What have we learned, where do we go from here?" *Tellus* (B), 44, 443-447, 1992.

Intergovernmental Panel on Climate Change (IPCC), *Climate Change 2001: The Scientific Basis,* Contribution of Working Group I to the Third Assessment Report of the IPCC, Cambridge University Press, New York, 2001.

Kasper-Giebl, A., A. Koch, R. Hitzenberger and H. Puxbaum, "Scavenging efficiency of 'aerosol carbon' and sulfate in super cooled clouds at Mt. Sonnblick (3106 m a.s.l., Austria),' *J. Atmos. Chem.,* 35, 33-46, 2000.

Kreidenweis,S.K., C. J. Walcek, G. Feingold, W. Gong, M.Z. Jacobson, C.-H. Kim, X. Liu, J.E. Penner, A. Nenes, J.H. Seinfeld "Modification of aerosol mass and size distribution due to aqueous-phase SO2 oxidation in clouds: Comparisons of several models," *J. Geophys. Res*., 108, (D7), 4213, doi:10.1029/2002JD002697, 2003.

Laj, P. et al., "Behavior of H2O2, NH3, and BC in mixed-phase clouds during CIME," *Atmos. Res.,* 58, 315-336, 2001.

Marshall, S.F., D.S. Covert and R.J. Charlson, "Relationship between asymmetry parameter and hemispheric backscatter ratio: implications for climate forcing by aerosols," *Appl. Opt.*, 34 (27), 6306-6311, 1995.

Noone, K. J., D. W. Johnson, et al. "A Case Study of Ship Track Formation in a Polluted Marine Boundary Layer." *J. Atmos. Sci.* 57(16): 2748-2764, 2000.

Noone, K.J., J.A. Ogren, A. Hallberg, H.C. Hansson, A. Wiedensohler, E. Swietlicki, "A statistical examination of the chemical differences between interstitial and scavenged aerosol," *Tellus* (B), 44, 581-592, 1992a

Noone, K.J., J.A. Ogren, A. Hallberg, J. Heintzenberg, J Strom, H-C Hansson, B. Svenningsson, A. Wiedensohler, S. Fuzzi, M.C. Facchini, B.G. Arends, A. Berner, "Changes in aerosol size- and phase distribution due to physical and chemical processes in fog," *Tellus* (B), 44, 489-504, 1992b.

Noone, K.J., R.J. Charlson, D.S. Covert, J.A.Ogren, J. Heintzenberg, "Cloud droplets: Solute concentration is size dependent," *J.Geophys. Res.*, 93, D8, 9477-9482, 1988.

Noone, K.J., Hansson, H-C, Mallant, R.K.A, "Droplet sampling efficiency from crosswinds:an inlet efficiency calibration," *J. Aerosol Sci.*, 23, 153-164, 1992

Ogren, J.A. and R.J. Charlson, "Elemental carbon in the atmosphere: cycle and lifetime," *Tellus* (B), 35, 241-254, 1983.

Ogren, J.A., J. Heintzenberg, R.J. Charlson, "In-situ sampling of clouds with a droplet to aerosol converter," *Geophys. Res. Lett.,* 12, 121-124, 1985.

Ogren, J.A., J. Heintzenberg, A. Zuber, K.J. Noone, R.J. Charlson, "Measurements of the size-dependence of solute concentrations in cloud droplets," *Tellus* (B), 42, 24-31, 1989.

Ogren, J.A., E. Andrews, D.S. Covert, K.J. Noone, "Effects of cloud scavenging on single scattering albedo," *Proceedings of the 14th International Conference on Clouds and Precipitation*, Bologna, Italy, July, 2004.

Quinn, P. K., Bates, T.S., Clarke, A.D., Wang, W., Rood, M., Andrews, E., Allan, J., Carrico, C.M., Coffman, D., "Impact of particulate organic matter on the relative humidity dependence of light scattering: A simplified parameterization," *Geophys. Res. Lett*., 32, L22809, doi:101029/2005GL024322, 2005.

Rosenfeld, D., "Suppression of rain and snow by urban and industrial air pollution", *Science*, 287, 1793-1796, 2000.

Twohy, C. H. and B. W. Gandrud, "Electron microscope analysis of residual particles from aircraft contrails." *Geophys. Res. Lett.,* 25(9), 1359-1362, 1998.

Wilson, J. C., and W. R. Seebaugh, "Measurement of Aerosol from Aircraft," Chapt. 30, Aerosol Measurement, 2nd Edition, Eds. P. Baron and K. Willeke, John Wiley & Sons, 2001:.